Food and Chemical Toxicology 133 (2019) 110767

Contents lists available at ScienceDirect

Food and Chemical Toxicology

journal homepage: www.elsevier.com/locate/foodchemtox

Effects of cyanidin-3-O-glucoside on 3-chloro-1,2-propanediol induced intestinal microbiota dysbiosis in rats

Guowei Chen[a,1], Gang Wang[b,1], Cuijuan Zhu[a], Xinwei Jiang[a], Jianxia Sun[c], Lingmin Tian[a,**], Weibin Bai[a,*]

[a] Department of Food Science and Engineering, Institute of Food Safety and Nutrition, Guangdong Engineering Technology Center of Food Safety Molecular Rapid Detection, Jinan University, Guangzhou, 510632, PR China
[b] Department of Neurosurgery, Nanfang Hospital Southern Medical University, Guangzhou, 510515, PR China
[c] School of Chemical Engineering and Light Industry, Guangdong University of Technology, Guangzhou, China

ARTICLE INFO

Keywords:
3-Chloro-1,2-propanediol
Cyanidin-3-O-Glucoside
Gut microbiota
Anthocyanin
Histopathological analysis
16s rDNA

ABSTRACT

Gastrointestinal studies suggested that balanced gut microbial community contribute to a healthy gut. Our previous studies have suggested that cyanidin-3-O-glucoside (C3G) can alleviate food contaminant 3-Chloro-1,2-propanediol (3-MCPD) induced testis injury and improve the spermatogenesis in rats. To the best of our knowledge, the effects of 3-MCPD exposure and C3G intervention on intestinal microbiota have not been studied. In the present study, male Wistar rats were used to investigate the effects of C3G and 3-MCPD on microbiota composition. After 3-MCPD treatment, the small intestinal showed histopathological alterations, including villus atrophy, necrosis, decreased number of epithelial cells and cellular infiltration. Supplementation of C3G brings the small intestine closer to normal histology. Meanwhile, 3-MCPD exposure significantly changed the diversity and composition of gut microbiota. At the phylum level, *Cyanobacteria* and *Firmicutes* were enriched in 3-MCPD groups, while *Actinobacteria* and *Proteobacteria* were decreased. Supplementation of C3G significantly increased the relative abundance of *Lachnospiraceae_NK4A136_group* and *Actinobacteria*, indicating that C3G may regulate the communities of gut microbiota towards a beneficial orientation. Our results indicate that C3G may protect the intestinal mucosa damage caused by 3-MCPD, and appropriate dose of C3G restrains gut microbial dysbiosis caused by 3-MCPD, which is a potential way to promote gut healthy.

1. Introduction

3-Chloro-1,2-propanediol (3-MCPD) is the most common chloropropanols in chemical food contaminants. It is primarily produced in foods during the hydrochloric acid assisted protein hydrolysis. As a byproduct of this process, chloride can react with the glycerol backbone of lipids to produce 3-MCPD (Tiong et al., 2018). 3-MCPD may also exist in food products which have been in contact with materials containing epichlorohydrin-based wet-strength resins (Hamlet et al., 2002). 3-MCPD was categorized by the International Agency for Research on Cancer as a potential carcinogenic component to humans (Commission, 2001).

The intake of 3-MCPD could result in development of nephrotoxicity in rats, testicular toxicity and carcinomas in male rats (Cho et al., 2008; Jiang et al., 2018), but no genotoxic potency (Aasa et al., 2017). Exposure to food contaminants, such as 2,3,7,8-tetrachlorodibenzofuran and 2,3,7,8-tetrachlorodibenzo-p-dioxin, led to changes of the gut microbial community and function in the hosts (Lefever et al., 2016; Zhang et al., 2015). Recently, the important roles of the gut microbiota in human health have attracted wide attention. Gastrointestinal studies suggested that balanced gut microbial community contribute to a healthy gut. Microbiota may alter the integrity of the intestinal barrier by regulating the innate immune system (Wan et al., 2018). To the best of our knowledge, the effects of 3-MCPD exposure on gut microbiota have not been studied. The gut microbiota is regarded as a new metabolic “organ” of the human body (Marchesi et al., 2016). Over time, alternation of intestinal microbiota has been identified as one of the main causes of chronic diseases, such as obesity, cerebrovascular disease, and fatty liver (Bruce-Keller et al., 2015; Cani et al., 2008; Koeth et al., 2013; Moreno-Navarrete et al., 2018).

** Corresponding author.
* Corresponding author.
E-mail addresses: tianlinmin@163.com (L. Tian), baiweibin@163.com (W. Bai).
[1] G. Chen and G. Wang contributed equally to this article.

https://doi.org/10.1016/j.fct.2019.110767
Received 9 July 2019; Received in revised form 14 August 2019; Accepted 16 August 2019
Available online 23 August 2019
0278-6915/ © 2019 Elsevier Ltd. All rights reserved.

Therefore, regulating intestinal microbiota is considered to be an important strategy to control chronic and metabolic diseases. Diet is a key modulator that could shift the imbalanced gut microbiota to a balanced state (Flint et al., 2012; Slavin, 2013; Tian et al., 2016).

Anthocyanins are group of polyphenols with significant antioxidant potential (Jiang et al., 2019). Our previous studies have suggested that anthocyanin can alleviate 3-MCPD induced testis injury and improve the spermatogenesis in male rats (Jiang et al., 2018). Vegetables and fruits are the main sources of anthocyanin intake. After ingestion, most of dietary anthocyanins (up to 65%) reach the colon intact and interact with the microbiota for biotransformation and metabolism before being absorbed by the intestinal mucosa (Jamar et al., 2017; Tian et al., 2018). However, there are few studies on the effects of Cyanidin-3-O-glucoside (C3G) alone or together with 3-MCPD on gut microbiota. In the present study, therefore, we used the highly purified C3G from black soybean coat and the rat model to investigate the possible effects of C3G and 3-MCPD on microbiota under environments of ileal contents, colonic contents and colonic mucosa. In addition, we evaluated small intestine and colon histopathology to explore the relationship between C3G, 3-MCPD and gut barrier.

2. Materials and methods

2.1. Chemicals and materials

The raw material black soybean coat was obtained from Anhui province, China. 3-MCPD was purchased from J&K Scientific, Beijing, China. The experimental diets were prepared according to the AIN-93 formula with or without C3G supplementation. All diets were prepared by Jiangsu medicine bio-pharmaceutical Co., Ltd. (Jiangsu China) and presented as pellets to the animals.

2.2. High purity C3G preparation and measurement

The extraction and purification of C3G from black soybean coats was following the method described in our previous study (Jiang et al., 2017). Briefly, acidic hydrous ethanol was used to obtain the crude extract from black soybean coat. The extract was loaded to macroporous absorption resin for obtaining the anthocyanin-rich fraction. Subsequently, mediumpressure liquid chromatography was used to acquire the highly purified C3G. The structure of C3G was identified using UPLC-MS/MS, and the purity (> 91.4%) was determined following the HPLC-PAD method.

2.3. Animal, diets, and sample preparation

40 male Wistar rats (13 weeks old), weight 403 ± 4 g were provided by the Medical Experimental Animal Center of Guangdong Province. After 10 days adaptation, the rats were randomly divided into 5 groups of 8 rats each. One group received saline and the standard diet (CONT group). One group received saline and a diet with supplementation of 500 mg/kg C3G (C3G-L group). The other three groups were treated with 3-MCPD through intragastric (ig.) administration at a dose of 20 mg/kg·bw per day. One of the three 3-MCPD treated groups received standard diet (3-MCPD group). In the two intervention groups, rats received 3-MCPD and C3G additive diet at two different doses of 500 mg/kg·diet (3-MCPD + C3G-L group) and 1000 mg/kg·diet (3-MCPD + C3G-H group) per day. The rats were kept in a SPF environment with a temperature of 23 ± 2 °C, a relative humidity of 50%–60%, and a light/dark cycle of 12 h. The rats had free access to food and water during the experiment. After 8 weeks treatment, all the animals were narcotized using pentobarbital sodium and sacrificed by cervical dislocation. Small intestine and colon of rats were taken and fixed with 4% paraformaldehyde immediately. The ileal and colonic contents were collected under super clean condition immediately. Then used a scalpel to scrape and collect colonic mucosa. All samples were stored in sterilized PE tubes and were freezed in liquid nitrogen immediately after the separation. All animal experiments are conducted in accordance with relevant laws and institutional guidelines. All experiments were accepted by the Animal Care and Protection Committee of Jinan University (Guangzhou, China).

2.4. Histopathological analysis

The small intestine and colon tissue of all rats were subjected to histopathological analysis. The samples that had been fixed and embedded in paraffin were then sectioned to slides with a thickness of 4 μm. The sections were stained using hematoxylin and eosin and then were subjected to analysis using light microscopy.

2.5. DNA extraction and amplification

Total DNA from the ileal and colonic contents and colonic mucosa of rats were extracted using DNA Extraction Kit (Life Technologies) following the manufacturer's instructions. Quality and quantity of DNA was verified with NanoDrop and agarose gel. Extracted DNA was diluted to a concentration of 1 ng/μl and stored at −20 °C until further processing. The diluted DNA was used as a template for PCR amplification of bacterial 16S rRNA genes with the barcoded primers and HiFi Hot Start Ready Mix (KAPA). For bacterial diversity analysis, V3–V4 variable regions of 16S rRNA genes was amplified with universal primers 343F (5′-TACGGRAGGCAGCAG-3′) and 798R (5′-AGGGTATCTA ATCCT-3′).

2.6. Library construction

Amplicon quality was visualized using gel electrophoresis, purified with AMPure XP beads (Agencourt), and amplified for another round of PCR. After purified with the AMPure XP beads again, the final amplicon was quantified using Qubit dsDNA assay kit. Equal amounts of purified amplicon were pooled for subsequent sequencing.

2.7. Sequence analysis

Raw sequencing data were in FASTQ format. Paired-end reads were then preprocessed using Trimmomatic software (Bolger et al., 2014) to detect and cut off ambiguous bases (N). It also cut off low quality sequences with average quality score below 20 using sliding window trimming approach. After trimming, paired-end reads were assembled using FLASH software (Reyon et al., 2012). Parameters of assembly were: 10bp of minimal overlapping, 200bp of maximum overlapping and 20% of maximum mismatch rate. Sequences were performed further denoising as follows: reads with ambiguous, homologous sequences or below 200bp were abandoned. Reads with 75% of bases above Q20 were retained. Then, reads with chimera were detected and removed. These two steps were achieved using QIIME software (version 1.8.0) (Caporaso et al., 2010).

Clean reads were subjected to primer sequences removal and clustering to generate operational taxonomic units (OTUs) using UPARSE software with 97% similarity cutoff (Edgar, 2013). The representative read of each OTU was selected using QIIME package. All representative reads were annotated and blasted against Silva database Version 123 (16s rDNA) using RDP classifier (confidence threshold was 70%) (Wang et al., 2007).

2.8. Statistical analysis

Graphpad Prism program was used to results analysis, and results are expressed as mean ± SEM. The data were analyzed using paired *t*-test. $p < 0.05$ was considered as statistically significant.

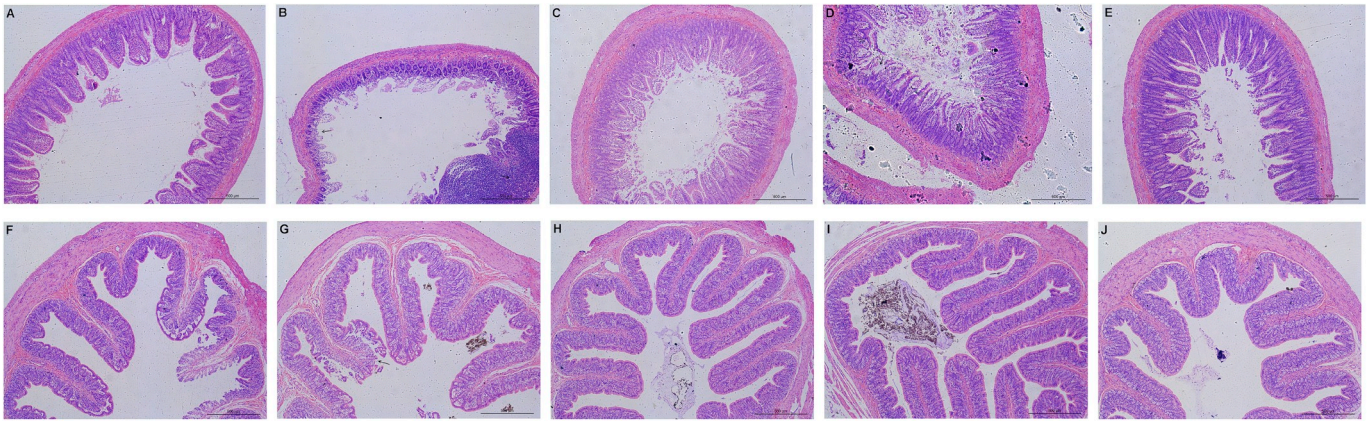

Fig. 1. Histopathological examination of small intestine (A, B, C, D and E) and colon (F, G, H, I and J) stained with hematoxylin-eosin.
(A) small intestine of CONT rats illustrating a normal mucosal architecture; (B) small intestine of 3-MCPD rats: villus atrophy, necrosis, decreased number of epithelial cells and an atrophic appearance in basal crypts, pronounced cellular infiltration; (C) small intestine of 3-MCPD + C3G-H rats illustrating nearly normal histology; (D) small intestine of 3-MCPD + C3G-L rats illustrating mild villus damage; (E) small intestine of C3G-L rats illustrating nearly normal histology. (F) colon of CONT rats illustrating a normal mucosal architecture; (G) colon of 3-MCPD rats illustrating villus damage; (H) colon of 3-MCPD + C3G-H rats illustrating nearly normal histology; (I) colon of 3-MCPD + C3G-L rats illustrating nearly normal histology; (J) colon of 3-C3G-L rats illustrating nearly normal histology. Bar expresses 500 μm.

3. Results

3.1. Effects of C3G on histopathological features of small intestine and colon

The histopathological images of the small intestine and colon are shown in Fig. 1. No pathological features were observed in the small intestine and colon of CONT rats (Fig. 1A and F). The villous height of the small intestine in the 3-MCPD group was significantly lower than that in the CONT group (Fig. 1B), whereas the villous height in the groups of 3-MCPD + C3G-H, 3-MCPD + C3G-L and C3G-L (Fig. 1C, D and E) was almost the same as that in the CONT group. In the 3-MCPD group, the integrity of the small intestine epithelium was destroyed. The villus atrophy, decreased number of epithelial cells, and an atrophic appearance in basal crypts were also observed in 3-MCPD group (Fig. 1B). In addition, 3-MCPD is less damaging to the colon than to the small intestine, and only causes damage to the colonic microvillus (Fig. 1G). The above histopathological changes were effectively ameliorated after treatment with the C3G (Fig. 1C and D for ileum and H, I for colon), and C3G-H showed better effect compared to C3G-L (Fig. 1C and H). In the groups without 3-MCPD intervention, C3G-L supplementation did not cause any histopathological change in both ileum (Fig. 1E) and colon (Fig. 1J).

3.2. Effects of C3G on microbial community in digesta and mucosa of rats without 3-MCPD ingestion

This study compared the overall differences of microbial communities at the OTU level. β-diversity were measured using a Nonmetric multidimensional scaling (NMDS) analysis-Unweighted UniFrac distances. Different colors in the figure represent different groups of samples. The results showed that the samples clustered based upon diet (Fig. 2). In the ileal and colonic contents, diet supplemented with 500 mg/kg C3G altered the composition of gut microbiota (Fig. 2A, 2B), but this change is not apparent in the colonic mucosa (Fig. 2C).

The α-diversity measure could indicate species richness and evenness within a sample. The rank abundance graph (Fig. 2D, 2E and 2F) showed that the most OTUs were showed low abundance in gut microbiota. Gut microbial α-diversity was defined by shannon index. The results showed that the shannon index of C3G-L group was significantly higher than CONT group in colonic contents ($p < 0.001$) (Table 1). There was no significant difference in shannon index of ileal contents and colonic mucosa microbiota, indicating that the uniformity and richness of the rats gut microbiota were significantly changed after C3G intervention in colonic contents.

Gut microbiota plays an important role in the pathogenesis of many diseases. We compared the difference of gut microbiota composition by 16S rRNA sequencing analysis. As shown in Fig. 3A, a total 15 phyla of gut microbiota was mainly composed of *Firmicutes*, *Proteobacteria*, *Bacteroidetes*, *Actinobacteria*, *Cyanobacteria*, *Tenericutes*, *Spirochaetae*, *Deferribacteres*, *Fusobacteria*, *Latescibacteria*, *Acidobacteria*, *Gemmatimonadetes*, *Nitrospirae*, *Lentisphaerae*, and *Fibrobacteres*. C3G modulated gut microbiota composition at the phylum level in the ileal contents, colon contents, and colonic mucosa are shown in Supporting Information Fig. 1A, 1B and 1C, respectively. Compared with the CONT group, the quantity of *Firmicutes* in colonic contents of C3G-L group was significantly increased ($p < 0.01$). The content of *Proteobacteria*, *Tenericutes* in colonic contents showed a significantly degressive ($p < 0.05$) after treatment with C3G-L. In ileal contents and colonic mucosa microbiota *Tenericutes* displayed a similar tendency, although no significant differences (Fig. 3A and Supporting Information Fig. 1A, 1B and 1C).

To further evaluate the changes of microbial community in the digesta and mucosa of rats, the 15 most abundant genera were listed in a graph. The result showed that the gut microbiota were mainly composed of *Bacteroides*, *Helicobacter*, *Romboutsia*, *Allobaculum*, *Desulfovibrio*, *Lachnospiraceae_NK4A136_group*, *Vibrio*, *Ruminococcaceae_UCG-005*, *Alloprevotella*, *Ruminiclostridium_9*, *Rothia*, *Anaerotruncus*, *Clostridium_sensu_stricto_1*, *Rikenellaceae_RC9_gut_group* and *Streptococcus* (Fig. 3B). The relative abundance differences of individual genus in the digesta samples between C3G-L group and CONT group are shown in Supporting Information Fig. 2A, B and C, respectively. In the ileal contents, the relative abundances of *Romboutsia*, *Lachnospiraceae_NK4A136_group* and *Rothia* were higher, and the abundance of *Bacteroides* and *Allobaculum* were lower in the C3G-L group compared with CONT group, although no significant differences (Fig. 3B and Supporting Information Fig. 2A). In the colonic contents, the relative abundance of *Allobaculum* ($p < 0.05$), *Lachnospiraceae_NK4A136_group* ($p < 0.001$) and *Anaerotruncus* ($p < 0.05$) was significantly increased, while *Bacteroides* ($p < 0.05$) and *Helicobacter* ($p < 0.05$) was significantly reduced in the C3G-L group compared with the CONT group (Fig. 3B and Supporting Information Fig. 2B). In the colonic mucosa, supplementation of C3G-L increased the relative abundance of *Lachnospiraceae_NK4A136_group*, *Ruminiclostridium_9* and

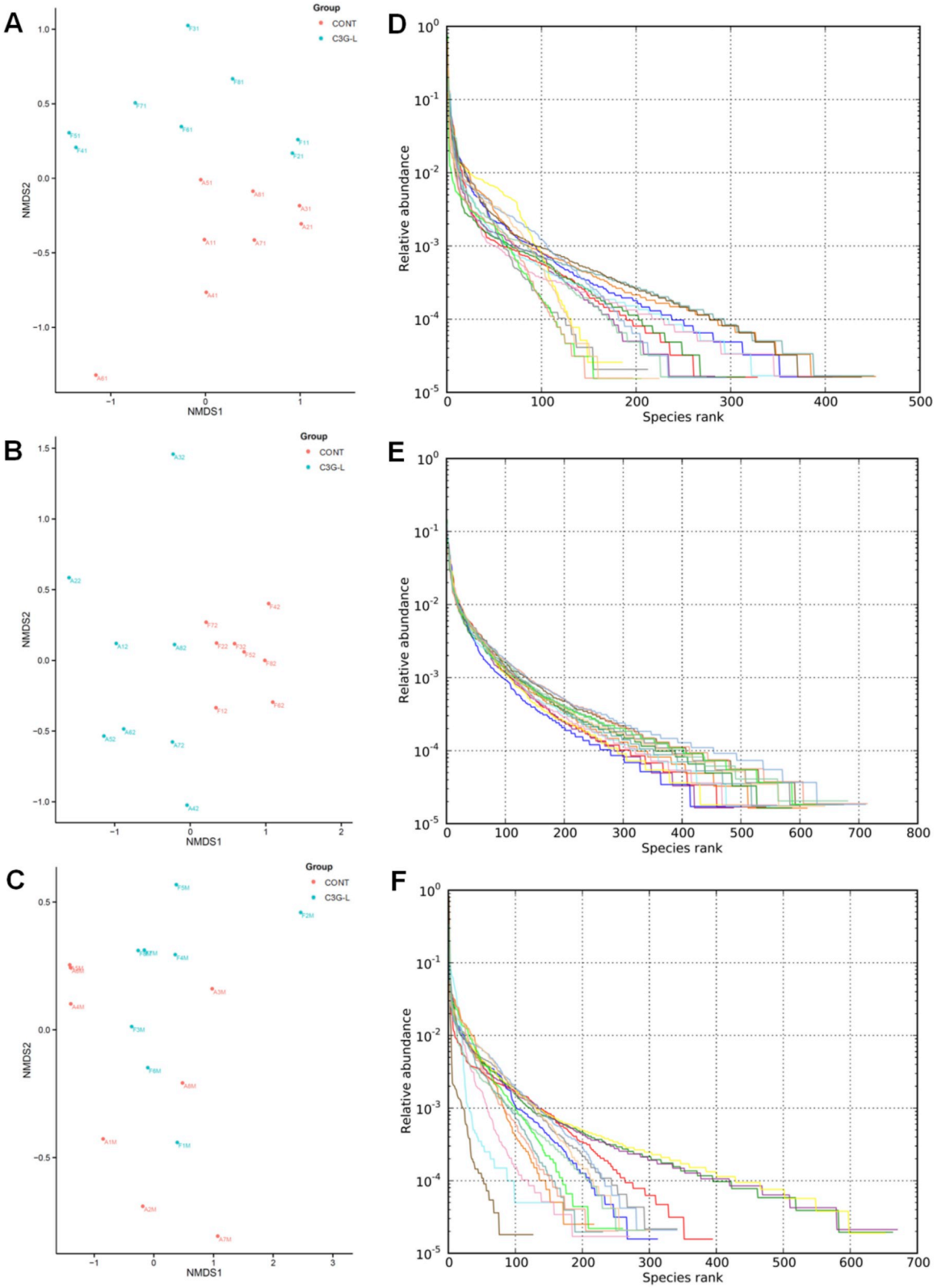

Fig. 2. Dietary C3G changes the structure of gut microbiota in rat without 3-MCPD ingestion. Nonmetric multidimensional scaling analysis (NMDS) plot of dietary effect by Unweighted UniFrac Distance in ileal contents (A), colonic contents (B) and colonic mucosa (C). Rank abundance curve of gut microbiota OTUs in ileal contents (D), colonic contents (E) and colonic mucosa (F).

Table 1
Comparison of Shannon diversity in the ileal digesta, colonic digesta and colonic mucosa of the rats in different groups.

Group	Ileal contents	Colonic contents	Colonic mucosa
CONT	4.71 ± 0.29	6.11 ± 0.06	5.70 ± 0.41
C3G-L	4.37 ± 0.40	6.62 ± 0.06***	5.23 ± 0.23
3-MCPD	4.77 ± 0.34	6.46 ± 0.08**	5.53 ± 0.23
3-MCPD + C3G-H	5.17 ± 0.36	6.60 ± 0.06	5.18 ± 0.40
3-MCPD + C3G-L	4.70 ± 0.45	6.74 ± 0.06#	5.17 ± 0.43

** means $p < 0.01$ and *** means $p < 0.001$ when compared with CONT group; # means $p < 0.05$ when compared with 3-MCPD group.

Lachnospiraceae_UCG-005 ($p < 0.05$), and decreased the relative abundance of *Bacteroides* and *Allobaculum* (Fig. 3B and Supporting Information Fig. 2B).

3.3. Effects of C3G on microbial community in digesta and mucosa of rats with 3-MCPD ingestion

The NMDS analyses are shown in Fig. 4. Different colors in the figure represent different groups of samples. For both ileal digesta and colonic mucosa, samples from rats fed with different diets could not be well clustered from each other (Fig. 4A and C). For colonic contents, samples from rats fed with 3-MCPD were almost separated from the ones from CONT, 3-MCPD + C3G-H and 3-MCPD + C3G-L groups (Fig. 4B). Colonic digesta samples from rats treated with 3-MCPD together with C3G were well separated from the control samples (Fig. 4B).

α-diversity analysis showed the highest microbial richness and evenness in colonic contents compared with ileal contents and colonic mucosa (Table 1). In addition, both 3-MCPD and C3G-L lead to an increase in the shannon index. The rank abundance graph (Fig. 4D. E and

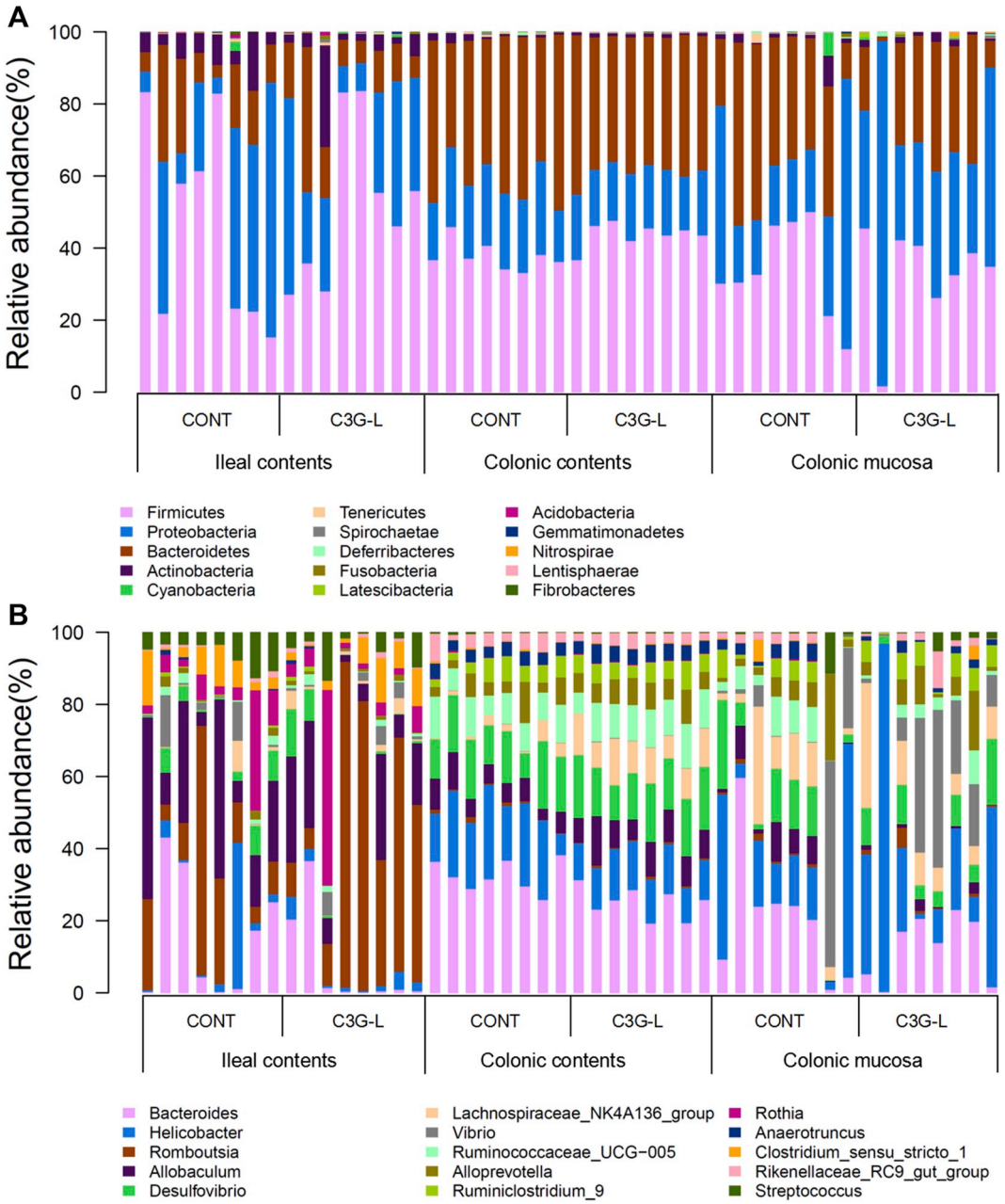

Fig. 3. Differential modulation of microbiota composition by C3G in rat without 3-MCPD ingestion. Bacterial community at the phylum-level (A) and at the genus level (B) in the ileal digesta, colonic digesta and colonic mucosa of the rats in different groups.

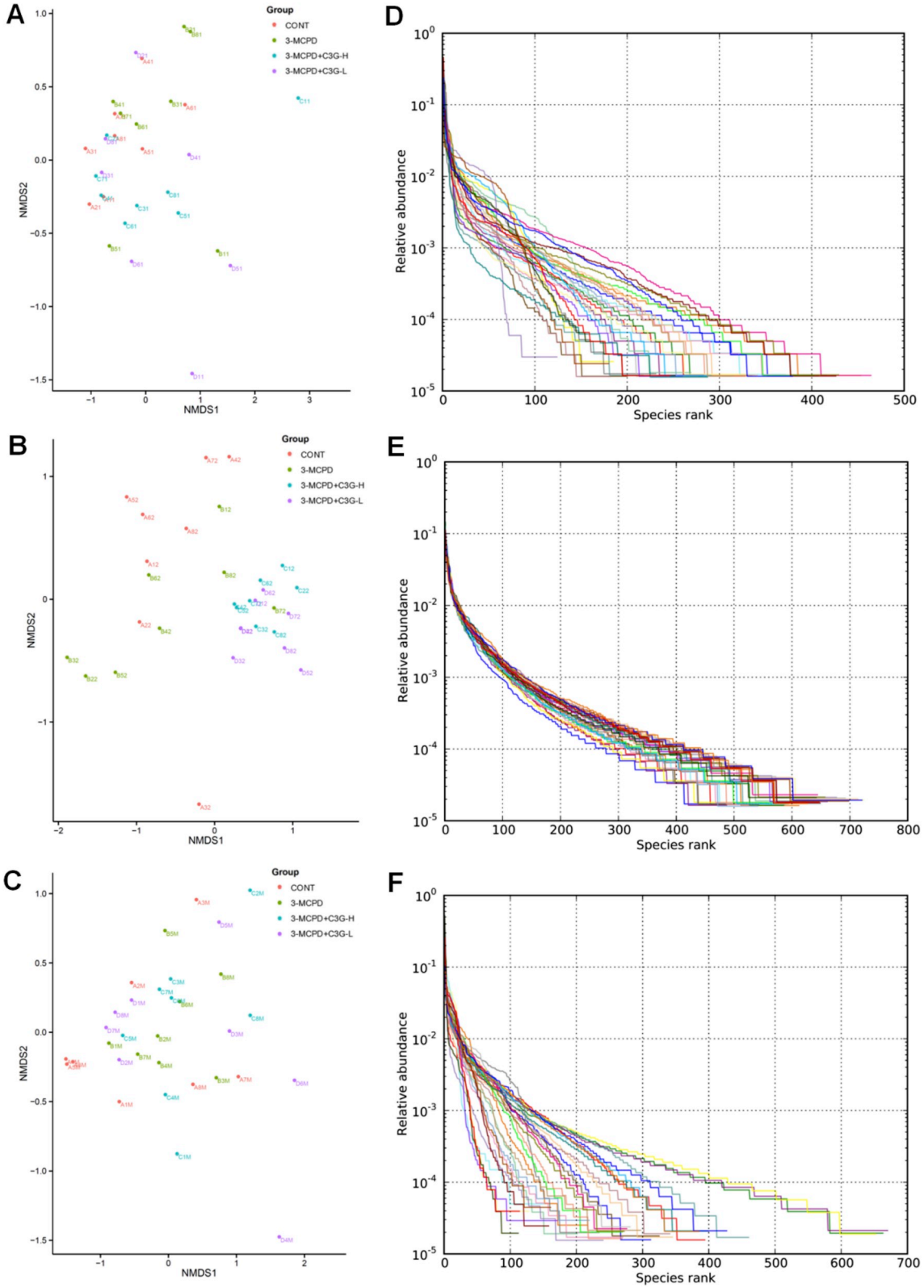

Fig. 4. Dietary C3G changes the structure of gut microbiota in rat with 3-MCPD ingestion. Nonmetric multidimensional scaling analysis (NMDS) plot of dietary effect by Unweighted UniFrac Distance in ileal contents (A), colonic contents (B) and colonic mucosa (C). Rank abundance curve of gut microbiota OTUs in ileal contents (D), colonic contents (E) and colonic mucosa (F).

F) also proved that most OTUs were showed low abundance in the gut microbiota.

At the phylum level, the gut microbiota consists of 15 major phyla: *Firmicutes*, *Proteobacteria*, *Bacteroidetes*, *Actinobacteria*, *Deferribacteres*, *Cyanobacteria*, *Tenericutes*, *Acidobacteria*, *Spirochaetae*, *Gemmatimonadetes*, *Fusobacteria*, *Latescibacteria*, *Lentisphaerae*, *JL-ETNP-Z39* and *Thaumarchaeota* (Fig. 5A). C3G modulated the 3-MCPD disrupted gut microbiota composition at the phylum level are shown in

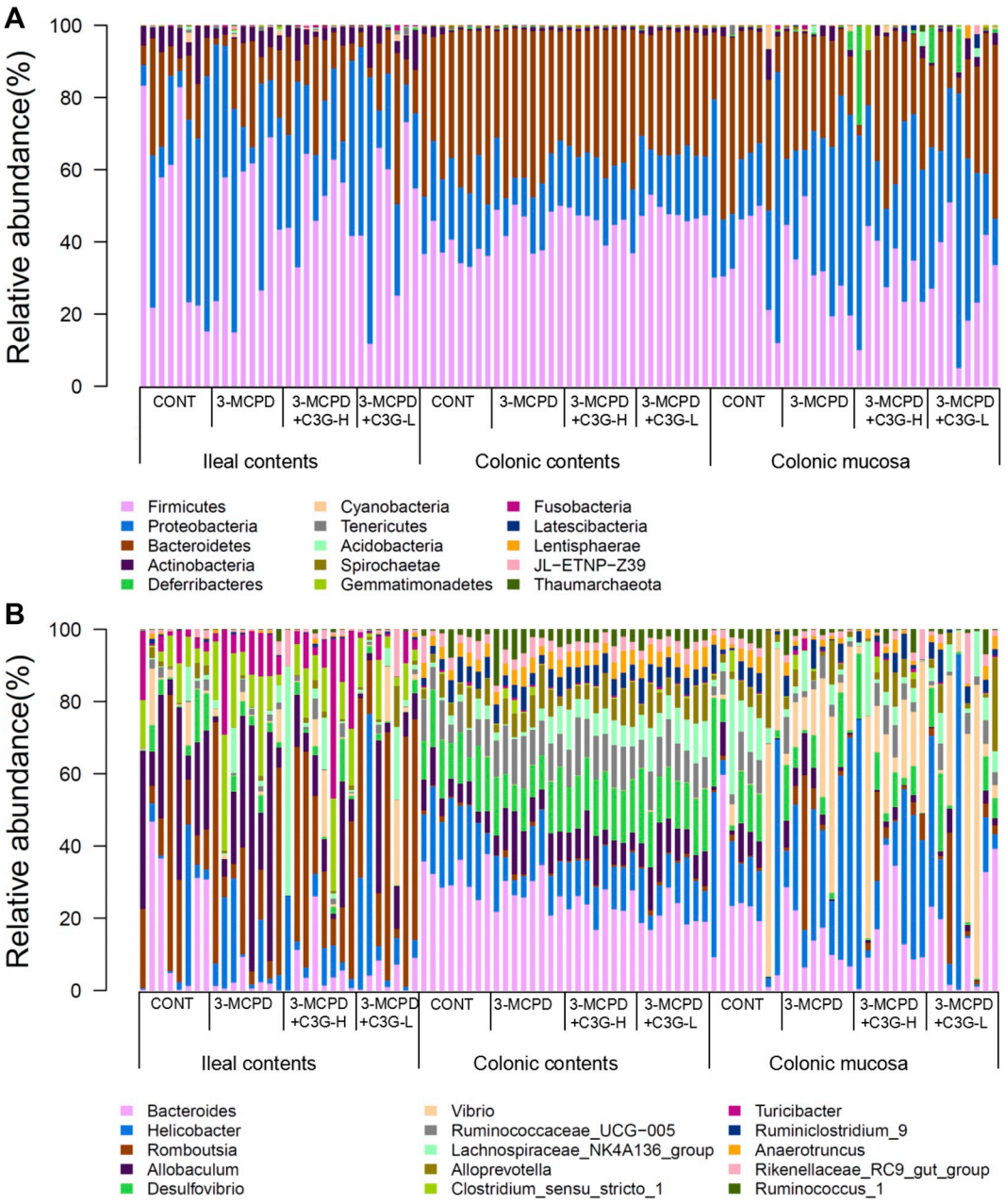

Fig. 5. Differential modulation of microbiota composition by C3G in rat with 3-MCPD ingestion. Bacterial community at the phylum-level (A) and at the genus level (B) in the ileal digesta, colonic digesta and colonic mucosa of the rats in different groups.

Supporting Information Fig. 1A, B and C, respectively. In ileal contents, *Actinobacteria* was reduced after 3-MCPD treatment. Compared with the 3-MCPD group, C3G-L supplementation increased *Actinobacteria* levels, although no significant differences (Fig. 5A; Supporting Information Fig. 1A). In colonic contents, *Firmicutes* was the incremental bacteria after 3-MCPD treatment, which relative content increasing from 37.72 ± 1.42 to 45.12 ± 1.97 ($p < 0.01$). And the content of *Proteobacteria* ($p < 0.05$) and *Actinobacteria* displayed a degressive trend. C3G-H and C3G-L supplementation reversed *Proteobacteria* levels. Supplementation with C3G-L significantly increased the relative abundance of *Actinobacteria* ($p < 0.05$) compared with the 3-MCPD group, whease *Bacteroidetes* ($p < 0.05$) was significantly decreased (Fig. 5A; Supporting Information Fig. 1B). In colonic mucosa, compared with the CONT group, the relative abundance of *Actinobacteria* displayed a reducing tendency in 3-MCPD group, but they were changed in the C3G-L group, although there was no significantly difference (Fig. 5A; Supporting Information Fig. 1C).

At the genus level, the gut microbiota were mainly consist of *Bacteroides*, *Helicobacter*, *Romboutsia*, *Allobaculum*, *Desulfovibrio*, *Vibrio*, *Ruminococcaceae_UCG-005*, *Lachnospiraceae_NK4A136_group*, *Alloprevotella*, *Clostridium_sensu_stricto_1*, *Turicibacter*, *Ruminiclostridium_9*, *Anaerotruncus*, *Rikenellaceae_RC9_gut_group* and *Ruminococcus_1* (Fig. 5B). C3G modulated the 3-MCPD disrupted gut microbiota composition at the genus level are shown in Supporting Information Fig. 2A, B and C, respectively. In ileal contents, compared with CONT group, 3-MCPD decreased the relative abundances of *Bacteroides*, *Rothia* and *Romboutsia*; and increased *Clostridium_sensu_stricto_1* (Fig. 5B and Supporting Information Fig. 2A). While supplement C3G increased the relative abundances of *Lachnospiraceae_NK4A136_group*, *Rothia*, *Romboutsia*; and decreased *Allobaculum* and *Clostridium_sensu_stricto_1*, although there was no significantly difference (Fig. 5B and Supporting Information Fig. 2A). In colonic contents, supplementation of C3G

reversed the changes in *Desulfovibrio* and *Ruminococcus_1* caused by 3-MCPD. Furthermore, 3-MCPD treatment significantly increased the relative abundance of *Ruminococcaceae_UCG-005* ($p < 0.05$), *Allobaculum* ($p < 0.05$), and decreased *Helicobacter* ($p < 0.05$). Supplementation with C3G-H ($p < 0.05$) and C3G-L ($p < 0.001$) significantly increased the relative abundance of *Lachnospiraceae_NK4A136_group* (Fig. 5B and Supporting Information Fig. 2B). In colonic mucosa, supplementation with C3G-H significantly decreased the relative abundance of *Allobaculum* ($p < 0.05$) and C3G-L increased *Lachnospiraceae_NK4A136_group* compared with 3-MCPD group (Fig. 5B and Supporting Information Fig. 2C). There was no significant difference in the regulation of gut microbiota between different doses of C3G.

4. Discussion

Effects of 3-MCPD and C3G on histopathological features of small intestine and colon. In the small intestine 3-MCPD is absorbed into plasma and involved in body circulation (Jędrkiewicz et al., 2016). The intestinal tract represents the first barrier against ingested food contaminants, as 3-MCPD, and has also an important role in immune functions (Turner, 2009). Previous studies have indicated that food contaminants, such as deoxynivalenol (Payros et al., 2017) and zearalenone (Liu et al., 2014) could cause villi loss and disruption in integrity of villi in mice and rats. In the present study, the damaging effects of 3-MCPD on small intestine and colon, evidenced by the histopathological features, was reported for the first time. Detailed evidences in related mRNA and protein expression needed to be further proved in the future. Disruption of the intestinal epithelial barrier may lead to inflame, further leading to bacterial translocation and other antigen entry. The protective mucous layer is the key to intestinal barrier function (Peng et al., 2019). We found that C3G has a protective effect on the damage of intestinal villus, microvillus and mucosa caused by 3-MCPD. Previous findings on pomegranate juice rich in anthocyanins also demonstrated its significant prevention on intestinal histopathological changes (Belal et al., 2009).

Effects of C3G on microbial community in digesta and mucosa of rats without 3-MCPD ingestion. Supplemented C3G caused a significant shift of microbiota composition in ileal and colonic digesta, but not in colonic mucosa. This could be due to the presence of abundant C3G in ileal (up to 85%) and colonic digesta (up to 65%) after ingestion (Tian et al., 2018). The quick utilization of C3G by gut microbiota present in the digesta may cause low amount of C3G reaching the mucosa. As a result, the microbiota present in the colonic mucosa was not significantly influenced. A remarkable increased *Firmicutes* and decreased *Proteobacteria* were detected in colonic digesta after C3G supplementation (Fig. 3A; Supporting Information Fig. 1B), compared with the CONT group. In contrast, OTU abundance of *Firmicutes* was decreased and OTU abundance of *Proteobacteria* was increased after supplementation of anthocyanin-rich fruit blueberry in mice (Lee et al., 2018). It could be due to the presence of other anthocyanin besides C3G in blueberry.

In the present study, we found that C3G supplementation increased the relative abundance of genera *Lachnospiraceae_NK4A136_group*, *Lachnospiraceae_UCG-005*, *Anaerotruncus*, *Romboutsia*, and *Ruminiclostridium_9* in phylum *Firmicutes*, and decreased the relative abundance of *Bacteroides* and *Helicobacter* in rats without 3-MCPD ingestion. Members of the *Lachnospiraceae* family, which is associated with maintaining intestinal health, may produce butyric acid to prevent colon cancer in humans (Xiao et al., 2019). More generally, it was shown that bilberry anthocyanin extract containing C3G increased the relative abundance of *Lachnospiraceae* and decreased the relative abundance of *Bacteroides* in aging rats (Li et al., 2019), in agreement with our findings. *Anaerotruncus* species may be the ideal probiotic strain, as it expresses enzymes that facilitate the production of butyric acid and also appear to play an active role in maintaining intestinal immune balance (Polansky et al., 2016). Recent study reported that the relative abundance of *Anaerotruncus* was increased by administration mulberry in which C3G is one of the main components (Hu et al., 2019).

Effects of C3G on microbial community in digesta and mucosa of rats with 3-MCPD ingestion. Since there is no report on intestinal microbiota change under 3-MCPD exposure, Wistar rat was used as a model to study the effects of continuous exposure to 3-MCPD on the intestinal microbiota. We found that exposure to food contaminant 3-MCPD caused shift in gut microbial community of rats. The colonic samples in 3-MCPD group were almost clustered separately from the colonic samples in CONT. However, the above differences were not observed significantly in the ileum and colonic mucosa. This could be due to the different microbiota composition in ileal digesta and the low amount of approachable 3-MCPD in colonic mucosa, respectively. We found that 3-MCPD exposure increased the relative abundances of phyla *Acidobacteria* and *Deferribacteres*, and decreased the relative abundances of *Actinobacteria*. To the best of our knowledge, neither the effect of 3-MCPD on the intestinal microbiota composition nor the metabolism of 3-MCPD by intestinal microbiota was not studied before. The decreased relative abundances of genera *Bacteroides*, *Rothia* and *Romboutsia*, and increased relative abundances of *Clostridium* and *Lachnospiraceae* after 3-MCPD ingestion were also reported in our present study for the first time.

The colonic samples in 3-MCPD + C3G-H and 3-MCPD + C3G-L groups were clearly clustered separately from those in CONT and 3-MCPD groups. However, no significant difference was found among the groups in the ileum and colonic mucosa. This may be due to the low bioavailability of anthocyanins, which are absorbed relatively little in the small intestine after ingestion (Cardona et al., 2013; Tian et al., 2018). Hence, most dietary anthocyanins reach the colon intact and are converted by the colonic microbiota into bioactive compounds before being absorbed by the colonic mucosa (Faria et al., 2014). Since gut microbiota dysbiosis is an important risk factor for animal disease (Mu et al., 2018), gut microbiota changes induced by 3-MCPD may have an adverse effect on rats. The present study showed that the decrease of *Rothia* and *Romboutsia* and increase of *Clostridium* induced by 3-MCPD ingestion were suppressed by the treatment with C3G. These results provide a theoretical basis for considering C3G or C3G-enriched food as a promising candidate for treating 3-MCPD induced microbiota dysbiosis.

5. Conclusions

3-MCPD exposure caused damage to the intestinal mucosa and significantly changed the diversity and composition of intestinal microbiota in male rats. Our results suggested that C3G may protect the intestinal mucosa damage caused by 3-MCPD, and appropriate dose of C3G ameliorates gut microbial dysbiosis caused by 3-MCPD, which is a potential way to promote gut healthy.

Conflicts of interest

The authors declare that there are no conflicts of interest.

Acknowledgments

This study was supported by the Natural Science Foundation of China (NSFC, No.31901706, No.31871816 and No.31771983), the Science and Technology Program of Guangzhou (201704020050, 201903010081), the Pearl River Talent Plan (2017GC010387), the Fundamental Research Funds for the Central Universities (21617324) and the Research Funds for Talented Scholars of Jinan University (88016675).

Appendix A. Supplementary data

Supplementary data to this article can be found online at https://doi.org/10.1016/j.fct.2019.110767.

References

Aasa, J., Törnqvist, M., Abramsson-Zetterberg, L., 2017. Measurement of micronuclei and internal dose in mice demonstrates that 3-monochloropropane-1,2-diol (3-MCPD) has no genotoxic potency in vivo. Food Chem. Toxicol. 109, 414–420. https://doi.org/10.1016/j.fct.2017.09.019.

Belal, S.K., Abdel-Rahman, A.H., Mohamed, D.S., Osman, H.E.H., Hassan, N.A., 2009. Protective effect of pomegranate fruit juice against aeromonas hydrophila-induced intestinal histopathological changes in mice. World Appl. Sci. J. 7, 245–254.

Bolger, A.M., Lohse, M., Usadel, B., 2014. Trimmomatic: a flexible trimmer for Illumina sequence data. Bioinformatics 30, 2114–2120. https://doi.org/10.1093/bioinformatics/btu170.

Bruce-Keller, A.J., Salbaum, J.M., Luo, M., Blanchard, E., Taylor, C.M., Welsh, D.A., Berthoud, H.R., 2015. Obese-type gut microbiota induce neurobehavioral changes in the absence of obesity. Biol. Psychiatry 77, 607–615. https://doi.org/10.1016/j.biopsych.2014.07.012.

Cani, P.D., Bibiloni, R., Knauf, C., Neyrinck, A.M., Neyrinck, A.M., Delzenne, N.M., Burcelin, R., 2008. Changes in gut microbiota control metabolic endotoxemia-induced inflammation in high-fat diet-induced obesity and diabetes in mice. Diabetes 57, 1470–1481. https://doi.org/10.2337/db07-1403.

Caporaso, J.G., Kuczynski, J., Stombaugh, J., Bittinger, K., Bushman, F.D., Costello, E.K., Fierer, N., Peña, A.G., Goodrich, J.K., Gordon, J.I., Huttley, G.A., Kelley, S.T., Knights, D., Koenig, J.E., Ley, R.E., Lozupone, C.A., McDonald, D., Muegge, B.D., Pirrung, M., Reeder, J., Sevinsky, J.R., Turnbaugh, P.J., Walters, W.A., Widmann, J., Yatsunenko, T., Zaneveld, J., Knight, R., 2010. QIIME allows analysis of high-throughput community sequencing data. Nat. Methods 7, 335–336. https://doi.org/10.1038/nmeth.f.303.

Cardona, F., Andrés-Lacueva, C., Tulipani, S., Tinahones, F.J., Queipo-Ortuño, M.I., 2013. Benefits of polyphenols on gut microbiota and implications in human health. J. Nutr. Biochem. 24, 1415–1422. https://doi.org/10.1016/j.jnutbio.2013.05.001.

Cho, W.S., Han, B.S., Nam, K.T., Park, K., Choi, M., Kim, S.H., Jeong, J., Jang, D.D., 2008. Carcinogenicity study of 3-monochloropropane-1,2-diol in Sprague-Dawley rats. Food Chem. Toxicol. 46, 3172–3177. https://doi.org/10.1016/j.fct.2008.07.003.

Commission, E., 2001. Opinion of the Scientific Committee on Food on 3-Monochloro-Propane-1, 2-diol (3-MCPD). EC Brussel, Belgium.

Edgar, R.C., 2013. UPARSE: highly accurate OTU sequences from microbial amplicon reads. Nat. Methods 10, 996–998. https://doi.org/10.1038/nmeth.2604.

Faria, A., Fernandes, I., Norberto, S., Mateus, N., Calhau, C., 2014. Interplay between anthocyanins and gut microbiota. J. Agric. Food Chem. 62, 6898–6902. https://doi.org/10.1021/jf501808a.

Flint, H.J., Scott, K.P., Louis, P., Duncan, S.H., 2012. The role of the gut microbiota in nutrition and health. Nat. Rev. Gastroenterol. Hepatol. 9, 577–589. https://doi.org/10.1038/nrgastro.2012.156.

Hamlet, C.G., Sadd, P.A., Crews, C., Velisek, J., Baxter, D.E., 2002. Occurrence of 3-chloro-propane-1,2-diol (3-MCPD) and related compounds in foods: a review. Food Addit. Contam. 19, 619–631. https://doi.org/10.1080/02652030210132391.

Hu, T.G., Wen, P., Fu, H.Z., Lin, G.Y., Liao, S.T., Zou, Y.X., 2019. Protective effect of mulberry (*Morus atropurpurea*) fruit against diphenoxylate-induced constipation in mice through the modulation of gut microbiota. Food Funct. 10, 1513–1528. https://doi.org/10.1039/c9fo00132h.

Jamar, G., Estadella, D., Pisani, L.P., 2017. Contribution of anthocyanin-rich foods in obesity control through gut microbiota interactions. Biofactors 43, 507–516. https://doi.org/10.1002/biof.1365.

Jędrkiewicz, R., Kupska, M., Głowacz, A., Gromadzka, J., Namieśnik, J., 2016. 3-MCPD: a worldwide problem of food chemistry. Crit. Rev. Food Sci. Nutr. 56, 2268–2277. https://doi.org/10.1080/10408398.2013.829414.

Jiang, X., Li, X., Zhu, C., Sun, J., Tian, L., Chen, W., Bai, W., 2019. The target cells of anthocyanins in metabolic syndrome. Crit. Rev. Food Sci. Nutr. 59, 921–946. https://doi.org/10.1080/10408398.2018.1491022.

Jiang, X., Shen, T., Tang, X., Yang, W., Guo, H., Ling, W., 2017. Cyanidin-3-O-beta-glucoside combined with its metabolite protocatechuic acid attenuated the activation of mice hepatic stellate cells. Food Funct. 8, 2945–2957. https://doi.org/10.1039/c7fo00265c.

Jiang, X., Zhu, C., Li, X., Sun, J., Tian, L., Bai, W., 2018. Cyanidin-3-o-glucoside at low doses protected against 3-chloro-1,2-propanediol induced testis injury and improved spermatogenesis in male rats. J. Agric. Food Chem. 66, 12675–12684. https://doi.org/10.1021/acs.jafc.8b04229.

Koeth, R.A., Wang, Z., Levison, B.S., Buffa, J.A., Org, E., Sheehy, B.T., Britt, E.B., Fu, X., Wu, Y., Li, L., Smith, J.D., DiDonato, J.A., Chen, J., Li, H., Wu, G.D., Lewis, J.D., Warrier, M., Brown, J.M., Krauss, R.M., Tang, W.H., Bushman, F.D., Lusis, A.J., Hazen, S.L., 2013. Intestinal microbiota metabolism of L-carnitine, a nutrient in red meat, promotes atherosclerosis. Nat. Med. 19, 576–585. https://doi.org/10.1038/nm.3145.

Lee, S., Keirsey, K.I., Kirkland, R., Grunewald, Z.I., Fischer, J.G., de La Serre, C.B., 2018. Blueberry supplementation influences the gut microbiota, inflammation, and insulin resistance in high-fat-diet-fed rats. J. Nutr. 148, 209–219. https://doi.org/10.1093/jn/nxx027.

Lefever, D.E., Xu, J., Chen, Y., Huang, G., Tamas, N., Guo, T.L., 2016. TCDD modulation of gut microbiome correlated with liver and immune toxicity in streptozotocin (STZ)-induced hyperglycemic mice. Toxicol. Appl. Pharmacol. 304, 48–58. https://doi.org/10.1016/j.taap.2016.05.016.

Li, J., Wu, T., Li, N., Wang, X., Chen, G., Lyu, X., 2019. Bilberry anthocyanin extract promotes intestinal barrier function and inhibits digestive enzyme activity by regulating the gut microbiota in aging rats. Food Funct. 10, 333–343. https://doi.org/10.1039/c8fo01962b.

Liu, M., Gao, R., Meng, Q., Zhang, Y., Bi, C., Shan, A., 2014. Toxic effects of maternal zearalenone exposure on intestinal oxidative stress, barrier function, immunological and morphological changes in rats. PLoS One 9, e106412. https://doi.org/10.1371/journal.pone.0106412.

Marchesi, J.R., Adams, D.H., Fava, F., Hermes, G.D.A., Hirschfield, G.M., Hold, G., Quraishi, M.N., Kinross, J., Smidt, H., Tuohy, K.M., Thomas, L.V., Zoetendal, E.G., Hart, A., 2016. The gut microbiota and host health: a new clinical frontier. Gut 65, 330–339. https://doi.org/10.1136/gutjnl-2015-309990.

Moreno-Navarrete, J.M., Serino, M., Blasco-Baque, V., Azalbert, V., Barton, R.H., Cardellini, M., Latorre, J., Ortega, F., Sabater-Masdeu, M., Burcelin, R., Dumas, M.E., Ricart, W., Federici, M., Fernández-Real, J.M., 2018. Gut microbiota interacts with markers of adipose tissue browning, insulin action and plasma acetate in morbid obesity. Mol. Nutr. Food Res. 62 (3). https://doi.org/10.1002/mnfr.201700721.

Mu, D., Meng, J., Bo, X., Wu, M., Xiao, H., Wang, H., 2018. The effect of cadmium exposure on diversity of intestinal microbial community of Rana chensinensis tadpoles. Ecotoxicol. Environ. Saf. 154, 6–12. https://doi.org/10.1016/j.ecoenv.2018.02.022.

Payros, D., Dobrindt, U., Martin, P., Secher, T., Bracarense, A.P.F., Boury, M., Laffitte, J., Pinton, P., Oswald, E., Oswald, I.P., 2017. The food contaminant deoxynivalenol exacerbates the genotoxicity of gut microbiota. mBio 8, e00007–17. https://doi.org/10.1128/mBio.00007-17.

Peng, Y., Yan, Y., Wan, P., Chen, D., Ding, Y., Ran, L., Mi, J., Lu, L., Zhang, Z., Li, X., Zeng, X., Cao, Y., 2019. Gut microbiota modulation and anti-inflammatory properties of anthocyanins from the fruits of *Lycium ruthenicum* Murray in dextran sodium sulfate-induced colitis in mice. Free Radic. Biol. Med. 136, 96–108. https://doi.org/10.1016/j.freeradbiomed.2019.04.005.

Polansky, O., Sekelova, Z., Faldynova, M., Sebkova, A., Sisak, F., Rychlik, I., 2016. Important metabolic pathways and biological processes expressed by chicken cecal microbiota. Appl. Environ. Microbiol. 82, 1569–1576. https://doi.org/10.1128/aem.03473-15.

Reyon, D., Tsai, S.Q., Khayter, C., Foden, J.A., Sander, J.D., Joung, J.K., 2012. FLASH assembly of TALENs for high-throughput genome editing. Nat. Biotechnol. 30, 460–465. https://doi.org/10.1038/nbt.2170.

Slavin, J., 2013. Fiber and prebiotics: mechanisms and health benefits. Nutrients 5, 1417–1435. https://doi.org/10.3390/nu5041417.

Tian, L., Scholte, J., Borewicz, K., van den Bogert, B., Smidt, H., Scheurink, A.J.W., Gruppen, H., Schols, H.A., 2016. Effects of pectin supplementation on the fermentation patterns of different structural carbohydrates in rats. Mol. Nutr. Food Res. 60, 2256–2266. https://doi.org/10.1002/mnfr.201600149.

Tian, L., Tan, Y., Chen, G., Wang, G., Sun, J., Ou, S., Chen, W., Bai, W., 2018. Metabolism of anthocyanins and consequent effects on the gut microbiota. Crit. Rev. Food Sci. Nutr. 59, 982–991. https://doi.org/10.1080/10408398.2018.1533517.

Tiong, S.H., Saparin, N., Teh, H.F., Ng, T.L.M., Md Zain, M.Z.B., Neoh, B.K., Md Noor, A., Tan, C.P., Lai, O.M., Appleton, D.R., 2018. Natural organochlorines as precursors of 3-monochloropropanediol esters in vegetable oils. J. Agric. Food Chem. 66, 999–1007. https://doi.org/10.1021/acs.jafc.7b04995.

Turner, J.R., 2009. Intestinal mucosal barrier function in health and disease. Nat. Rev. Immunol. 9, 799–809. https://doi.org/10.1038/nri2653.

Wan, M.L.Y., Ling, K.H., El-Nezami, H., Wang, M.F., 2018. Influence of functional food components on gut health. Crit. Rev. Food Sci. Nutr. 59, 1927–1936. https://doi.org/10.1080/10408398.2018.1433629.

Wang, Q., Garrity, G.M., Tiedje, J.M., Cole, J.R., 2007. Naive Bayesian classifier for rapid assignment of rRNA sequences into the new bacterial taxonomy. Appl. Environ. Microbiol. 73, 5261–5267. https://doi.org/10.1128/AEM.00062-07.

Xiao, L., Chen, B., Feng, D., Yang, T., Li, T., Chen, J., 2019. TLR4 may be involved in the regulation of colonic mucosal microbiota by vitamin A. Front. Microbiol. 10, 268. https://doi.org/10.3389/fmicb.2019.00268.

Zhang, L., Nichols, R.G., Correll, J., Murray, I.A., Tanaka, N., Smith, P.B., Hubbard, T.D., Sebastian, A., Albert, I., Hatzakis, E., Gonzalez, F.J., Perdew, G.H., Patterson, A.D., 2015. Persistent organic pollutants modify gut microbiota–host metabolic homeostasis in mice through aryl hydrocarbon receptor activation. Environ. Health Perspect. 123, 679–688. https://doi.org/10.1289/ehp.1409055.